Organic & Biomolecular Chemistry

PAPER

View Article Online
View Journal

Cite this: DOI: 10.1039/c8ob03150a

Enzymatic radiosynthesis of a ^{18}F-Glu-Ureido-Lys ligand for the prostate-specific membrane antigen (PSMA)†

Phillip T. Lowe, [a] Sergio Dall'Angelo, [b] Ian N. Fleming, [c] Monica Piras, [b] Matteo Zanda *[b,d] and David O'Hagan *[a]

Prostate cancer represents a major public health threat as it is one of the most common male cancers worldwide. The prostate-specific membrane antigen (PSMA) is highly over-expressed in prostatic cancer cells in a manner that correlates with both tumour stage and clinical outcome. As such, PSMA has been identified as an attractive target for both imaging and treatment of prostate cancer. In recent years the focus on urea-based peptidomimetic inhibitors of the PSMA (representing low molecular weight/high affinity binders) has intensified as they have found use in the clinical imaging of prostate tumours. Reported herein are the design, synthesis and evaluation of a new fluorinated PSMA targeting small-molecule, FDA-PEG-GUL, which possesses the Glu-NH-CO-NH-Lys pharmacophore conjugated to a 5′-fluorodeoxy-adenosine unit. Inhibition assays were performed with FDA-PEG-GUL which revealed that it inhibits the PSMA in the nanomolar range. Additionally, it has been purposely designed so that it can be produced using the fluorinase enzyme from its chlorinated precursor, allowing for the enzymatic synthesis of radiolabelled [^{18}F]FDA-PEG-GUL *via* a nucleophilic reaction that takes place in experimentally advantageous conditions (in water at neutral pH and at ambient temperature). Specific binding of [^{18}F]FDA-PEG-GUL to PSMA expressing cancer cells was demonstrated, validating it as a promising PSMA diagnostic tool. This work establishes a successful substrate scope expansion for the fluorinase and demonstrates its first application towards targeting the PSMA.

Received 19th December 2018,
Accepted 17th January 2019

DOI: 10.1039/c8ob03150a

rsc.li/obc

Introduction

Prostate cancer represents one of the most common malignancies in men and is diagnosed annually in over 1 million patients worldwide.[1] With a substantial morbidity and mortality rate, it is a major public health issue.[2] The selection of appropriate treatments using diagnosis derived from high resolution imaging is therefore of the foremost importance.[2,3] The prostate-specific membrane antigen (PSMA), also known as glutamate carboxypetidase II, *N*-acetyl-α-linked acidic dipeptidase I (Naaladase I) or folate hydrolase, is a type II zinc dependant integral membrane protein that is overexpressed in almost all prostate cancers.[4–6] PSMA catalyses the hydrolysis of *N*-acetylaspartylglutamate (NAAG) to generate glutamate and *N*-acetylaspartate (NAA),[7,8] the excessive production of which has been linked to a number of health issues including a variety of neurological diseases.[9,10] Primarily restricted to the prostate, PSMA expression levels in cancerous cells are approximately 1000 times higher than that of healthy tissue in other organs (such as those of the kidney and small intestine).[11] Significantly, its expression correlates with both the stage and grade of the tumour progression;[12,13] due to each of these factors, PSMA has become an increasingly important diagnostic and therapeutic target.[10,14–16]

Numerous low molecular weight PSMA inhibitors derived from NAAG have been developed,[17] with 2-(phosphonomethyl)-pentandioic acid (2-PMPA)[18] being the first potent inhibitor synthesised. Subsequently a number of thiol,[19] indole[20] and hydroxamate[21] derivatives were designed, see Fig. 1. Of particular interest in recent years has been a class of urea-based inhibitors which possess the Glu-NH-CO-NH-Lys/Glu (GUL/GUG) pharmacophore.[10,17,22] A number of compounds of this class have shown improved potency as PSMA

[a]School of Chemistry and Biomedical Sciences Research Centre, University of St Andrews, North Haugh, St Andrews KY16 9ST, UK. E-mail: do1@st-andrews.ac.uk
[b]John Mallard Scottish PET Centre School of Medicine, Medical Sciences and Nutrition University of Aberdeen, Foresterhill, Aberdeen, AB25 2ZD, UK. E-mail: m.zanda@abdn.ac.uk
[c]Aberdeen Biomedical Imaging Centre, Institute of Medical Sciences Foresterhill, Aberdeen, AB25 2ZD, UK
[d]C.N.R. – I.C.R.M., via Mancinelli 7, 20131 Milan, Italy

†Electronic supplementary information (ESI) available: Compound synthesis and characterisation, assay conditions and fluorinase overexpression and purification. See DOI: 10.1039/c8ob03150a

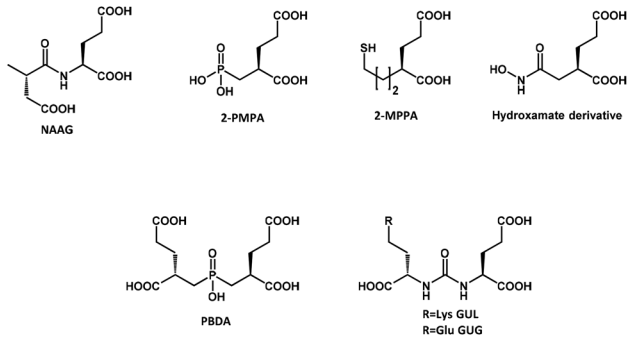

Fig. 1 The PSMA substrate *N*-acetylaspartylglutamate (NAAG) and examples of low-molecule-based PSMA inhibitors.

inhibitors. Their relative synthetic accessibility and inherent modularity have permitted many of these inhibitors to be modified for use in clinical imaging modalities *via* incorporation of various radioisotopes.[23–27]

Due to its high sensitivity, positron emission tomography (PET)[28] has emerged as a valuable tool for imaging prostate cancer using radiolabelled urea-based inhibitors of PSMA. With its moderate half-life ($t_{1/2}$ = 109.8 min, affording sufficient time for radioisotope incorporation), short positron range (2.3 mm in water, allowing for high resolution images) and ease of production (with availability at any PET facility in possession of a cyclotron) [^{18}F]fluoride is a preferred isotope for PET imaging.[28] Thus, incorporation of [^{18}F]fluoride into urea-based inhibitors represents a potentially valuable tool for imaging prostate tumours.[29] To date, methods to integrate [^{18}F]fluoride into these compounds have been developed using indirect, multistep strategies involving the initial synthesis of a ^{18}F-labelled prosthetic group such as [^{18}F]fluorobenzaldehyde ([^{18}F]FBA) or 2,3,5,6-tetrafluorophenylester-6-[^{18}F]-fluoronicotinate ([^{18}F]FPyl-TFP), which are then conjugated to the urea based inhibitor.[30,31] Such a strategy has been applied to the synthesis of [^{18}F]DCFPyl and [^{18}F]PSMA-1007, both of which have shown promise during preclinical investigation.[31] Alternatively, direct radiolabelling of urea-based inhibitors *via* [^{18}F]AlF-complexation is also being investigated and has been used for the synthesis of Al[^{18}F]PSMA-HBED;[32–34] once optimised, such a strategy may provide a potentially more efficient route to radio-fluorinated PSMA tracers for clinical application. As such, new [^{18}F]fluoride-radiotracers possessing the Glu-NH-CO-NH-Lys/Glu pharmacophore, along with the development of novel methodology to incorporate the [^{18}F]fluoride ion into these motifs, is of great interest.

The fluorinase enzyme, originally isolated from *Streptomyces cattleya*,[35] mediates the conversion of fluoride ion and *S*-adenosyl-L-methionine (AdoMet) to 5′-fluoro-5′-deoxyadenosine (5′-FDA) and L-methionine (L-Met), Scheme 1.[36] Furthermore, it can also utilise L-Met (or L-SeMet) in the reverse direction and catalyse the displacement of chloride from 5′-chloro-5′-deoxyadenosine (5′-ClDA) to generate AdoMet (or AdoSeMet), which allows for an overall transhalogenation reaction to occur if fluoride is present (Scheme 1).[37] The fluorinase enzyme has been shown to possess a distinct localised tolerance in its substrate promiscuity, allowing for decoration of the C-2 position of the adenine ring of 5′-ClDA with extensively functionalised acetylene substituents.[38] This promiscuity offers the opportunity to exploit its function to accommodate the direct ^{18}F-radiolabelling of biologically relevant molecules to generate chemically stable C–^{18}F bonds under aqueous ambient conditions at near-neutral pH. In this manner, the fluorinase offers advantage when compared to many other radiolabelling methodologies, as its activity in aqueous environments circumvents the requirement to secure anhydrous [^{18}F]fluoride *via* ion-exchange chromatography and as a Kryptofix® [2,2,2] formulation. The enzyme has the additional benefits of not requiring the use of protecting groups, increased temperatures or high/low pH levels. Furthermore, conventional HPLC methodology can be used to separate non-radiolabelled starting material from radiolabelled product, regardless of the targeting scaffold tethered to the fluorinase binding motif. To date, this late-stage enzymatic ^{18}F-radiolabelling has been accomplished with cancer targeting pegylated RGD peptides[38–40] and A2A adenosine receptor agonists,[41] as well as tetrazine and biotin motifs,[42] for use as radiotracers in PET.

For this study we have designed and synthesised a ClDA-PEG-GUL **15** construct to be used as a novel substrate for the fluorinase enzyme. It is designed as such to encompass both a 5′-chloro-5′-deoxyadenosine unit (responsible for binding to the fluorinase active site and undergoing an overall fluorination), a PEGylated spacer unit (to project tethered cargo away from the enzyme) and a PSMA binding GUL tethered to the terminus of the PEG unit through amide coupling, see Scheme 2. ClDA-PEG-GUL **15** has been utilised in a fluorinase mediated transhalogenation reaction to generate its

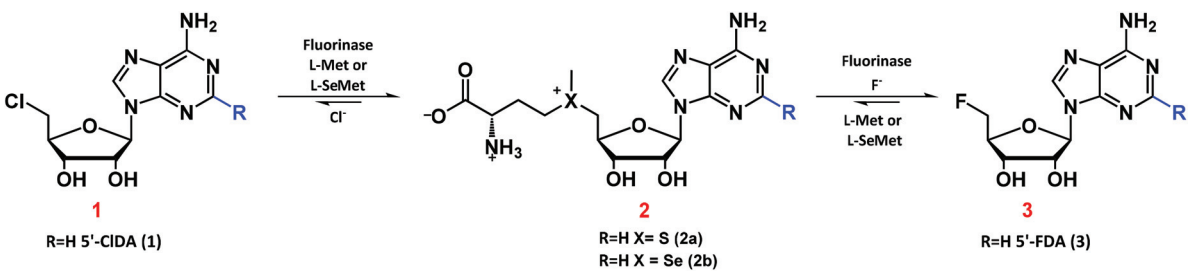

Scheme 1 Fluorinase-catalysed transhalogenation reactions with C-2 modified 5′-chloro-5′-deoxyadenosine substrates.

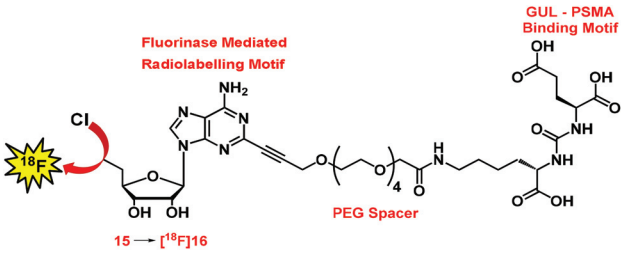

Scheme 2 Design of the last step ^{18}F-radiolabelling strategy of ClDA-PEG-GUL.

fluorinated analogue FDA-PEG-GUL **16**, which was subsequently assessed *in vitro* for its ability to inhibit the PSMA protein.

Results and discussion

Synthesis of ClDA-PEG-GUL 15

The synthesis of ClDA-PEG-GUL **15** was accomplished using a three-step approach (Scheme 3B) to allow for the individual synthesis and then successive coupling of each component required to assemble the substrate. These components are the ClDA binding moiety, the functionalised PEG spacer and the GUL PSMA binding motif. Firstly, the synthesis of the Glu-NH-CO-NH-Lys 7 (Scheme 3A) was achieved in a three-step

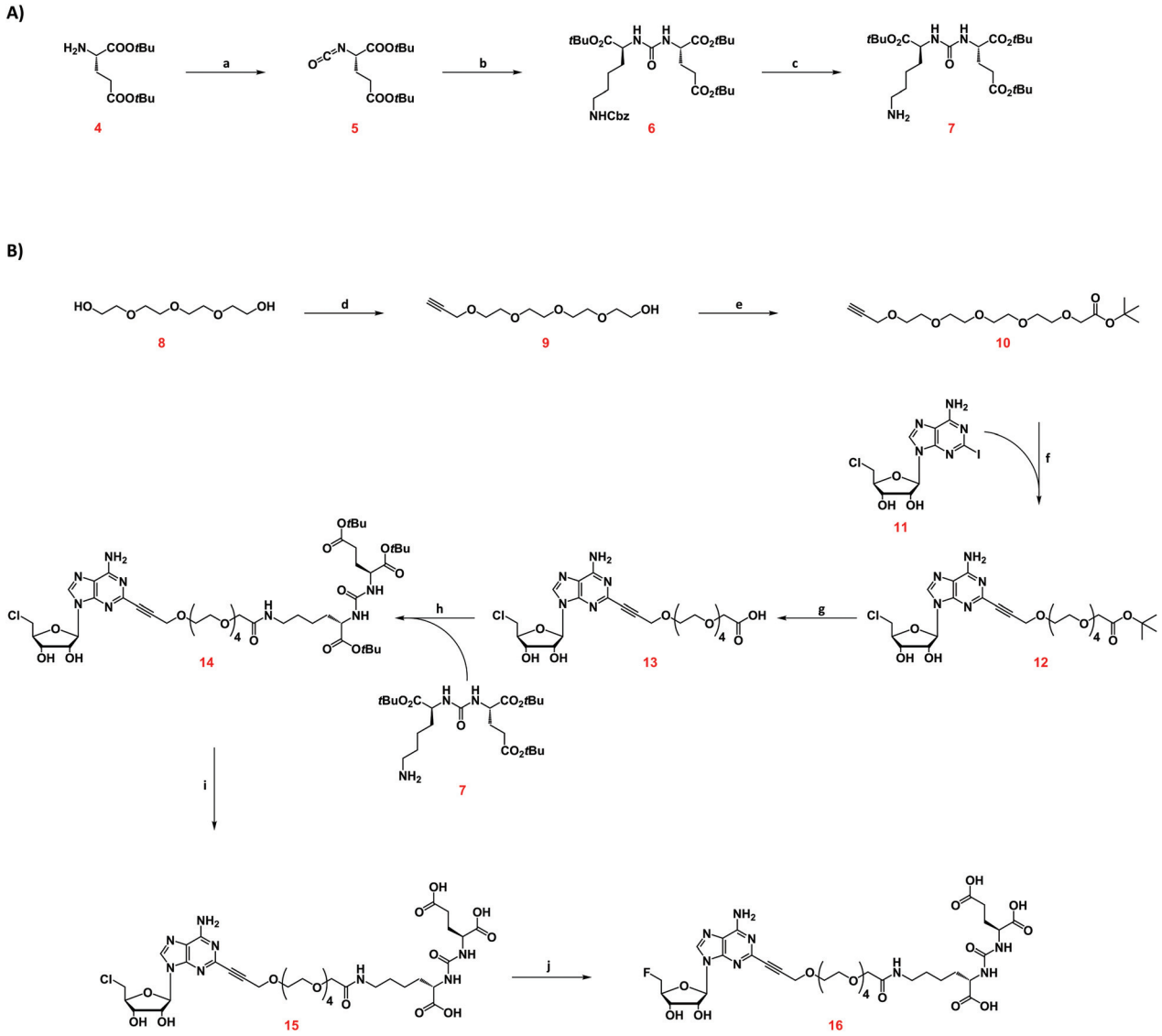

Scheme 3 (A) Synthesis of (*t*-butyl protected)GUL **14**. (B) Synthesis of ClDA-PEG-GUL **15** and FDA-PEG-GUL **16**. Reagents and conditions: (a) Triphosgene, DCM/$NaHCO_3$ sat., 99%; (b) H-Lys(Cbz)-O*t*Bu·HCl pyridine, DCM, 77%; (c) H_2, $Pd(OH)_2$, MeOH, 99%; (d) THF, NaH, propargyl bromide, 58%; (e) THF, NaH, *tert*-butyl bromoacetate, 60%; (f) $Pd_2(dba)_3$, Et_3N, CuI, DMF, 59%; (g) TFA, DCM, 98%; (h) PyBOP, DIPEA, DMF, 42%; (i)TFA, DCM, 57%; (j); fluorinase, L-SeMet, KF, phosphate buffer (pH 7.8), 70%.

manner from H-Glu(*Ot*BU)-O*t*Bu **4**. Briefly, **4** was treated with triphosgene under basic conditions to afford isocyanate intermediate **5**, which was used directly in subsequent coupling reactions, without the need for further purification. Isocyanate **5** was then reacted with H-Lys(Cbz)-O*t*Bu in the presence of pyridine to afford the fully protected peptidomimetic **6** in good yield after flash chromatography. Finally, the Cbz protecting group was removed *via* hydrogenation to yield (*t*-butyl protected) GUL **7**, which was used in subsequent coupling reactions without further purification. The synthesis of the 5′-chlorodeoxy-2-iodo-adenosine **11** was achieved *via* a five-step protocol using previously established methods[39] and the alkyne/protected carboxylate functionalised linker **10** was obtained *via* a two-step process.[42]

With **7**, **10** and **11** in hand, their assembly was addressed. Firstly **10** and **11** were combined *via* a Sonogashira cross-coupling reaction, which, after successive flash chromatography and C18 cartridge purification, afforded **12** in good yield. *tert*-Butyl ester **12** was then deprotected with TFA to afford the corresponding carboxylic acid **13**. Carboxylic acid **13** was then utilised in a peptide coupling reaction using an excess of **7**, PYBOP and DIPEA to generate ClDA-PEG-(*t*-butyl protected) GUL **14** in good yield after purification by semi-prep HPLC (Scheme 3B). Finally, the *tert*-butyl groups of ClDA-PEG-(protected)GUL **14** were removed by TFA. Particular care was taken during this procedure and the reaction was monitored by analytical HPLC to ensure unnecessarily long reaction times were avoided (see ESI†). Semi-preparative HPLC was then used to provide the candidate fluorinase substrate ClDA-PEG-GUL **15** in good yield (70%) and high purity (>95%.).

Fluorinase mediated transhalogenation of ClDA-PEG-GUL 15

In order to establish whether ClDA-PEG-GUL **15** can undergo biotransformation to its fluorinated analogue, small scale analytical transhalogenation reactions were performed. Accordingly, ClDA-PEG-GUL **15** was incubated in aqueous buffered media (pH 7.8) with the fluorinase (1 mg mL^{-1}), L-SeMet and KF (see ESI† for full experimental detail) and reaction progress was monitored by analytical HPLC over a period of 48 h. The time course profile generated from this assay revealed that **15** was an efficient substrate for the fluorinase with a 40% conversion between 0–1 h, at which point FDA-PEG-GUL **16** production levels off (reaching 60% in 4 h and ~90% in 10 h), see Fig. 2. This data reveals that the GUL motif does not interfere with the ability of the fluorinase to perform an overall transhalogenation from ClDA-PEG-GUL. Importantly, no degradation of ClDA-PEG-GUL **15** or the fluorinated FDA-PEG-GUL **16** product was observed during these assays.

A larger scale transhalogenation reaction was then performed to allow for the acquisition of FDA-PEG-GUL in order to evaluate its ability to bind and inhibit PSMA. The reaction was carried out on a ~3 mg scale and monitored by HPLC. After a 90% conversion, the protein was precipitated by heating and the reaction centrifuged in an eppendorf. Purification of the lysate was accomplished using semi-prep HPLC to afford **16** (~2 mg) in high purity.

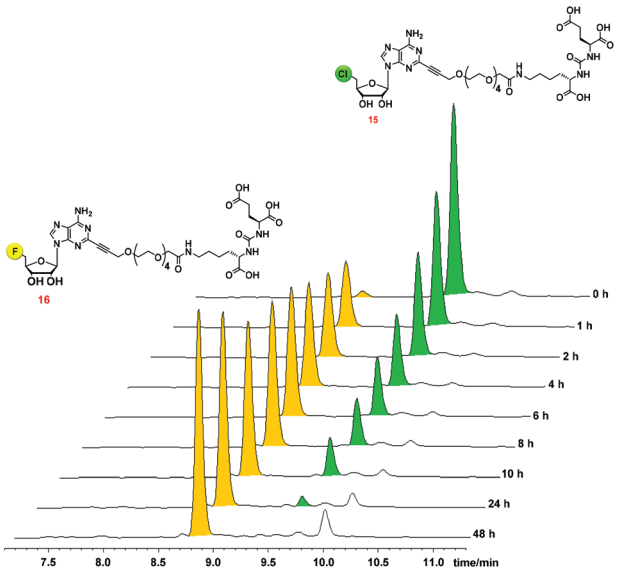

Fig. 2 HPLC time course (UV, 254 nm) of the incubation of ClDA-PEG-GUL **15**, green (t_R = 9.5 min), with the fluorinase, L-SeMet, KF, phosphate buffer (pH 7.8) at 37 °C. Traces show the formation of FDA-PEG-GUL **16**, yellow (t_R = 8.8 min), and the consumption of ClDA-PEG-GUL **15**. For full conditions see the Experimental section and ESI.†

Evaluation of 16 as an inhibitor of PSMA

The ability of FDA-PEG-GUL **16** to inhibit PSMA activity was determined using a fluorescence-based assay, essentially as previously reported.[43] Briefly, purified recombinant human PSMA protein was incubated with each test compound in the presence of *N*-acetylaspartylglutamate as the substrate, at 37 °C for 60 min. The reaction was then stopped by heating at 95 °C for 5 min and the resulting solution incubated with a solution of *ortho*-phthaldialdehyde (OPA, 15 mM) in OPA buffer (0.2 M NaOH and 0.1% (v/v) β-mercaptoethanol) for 10 min at room temperature. Aliquots were then assessed for fluorescence in a microplate reader using an excitation wavelength of 330 nm and an absorption wavelength of 450 nm, to determine the amount of free glutamate present. The binding affinity of each test compound to purified recombinant human PSMA was expressed as its 50% inhibitory concentration (IC_{50} value) in the assay (IC_{50} values were calculated using GraphPad Prism 5, see ESI† for full experimental detail).

FDA-PEG-GUL **16** and 2-PMPA were both tested in the assay. As expected,[44] 2-PMPA was a potent PSMA inhibitor, exhibiting an IC_{50} value of 18 nM in this assay (Table 1). The fluorine containing **16** was also a similarly good PSMA inhibitor, with an IC_{50} value in the nanomolar range. These data establish that **16** binds PSMA with high affinity.

Radiosynthesis of [^{18}F]FDA-PEG-GUL ([^{18}F]16)

A protocol was developed to enzymatically radiolabel the prospective radiotracer [^{18}F]FDA-PEG-GUL ([^{18}F]**16**). Briefly, for hot labelling experiments using the fluorinase enzyme, [^{18}F] fluoride was generated in an [$^{18}OH_2$] aqueous solution at GBq

Table 1 IC_{50} values of selected PSMA analogues were measured for their ability to compete with a standard glutamate containing peptide (Ac-Asp-Glu) as substrate for purified recombinant human PSMA enzyme. Results are the average ± standard error (s.e.) from three independent experiments, each performed in triplicate

Compound	IC_{50} ± s.e. (nM)
FDA-PEG-GUL 16	98.6 ± 22.5
2-PMPA	18 ± 5.0

levels. An aliquot of this (MBq of [^{18}F]fluoride, picomolar levels) was then added to a buffered solution (pH 7.8) of **15**, L-SeMet and a considerable excess of fluorinase enzyme (micromolar, see Experimental section), and the reaction mixture was incubated at 37 °C. For this protocol, the stoichiometry of the radiolabelling biotransformation reaction is dramatically reversed with respect to the non-radioactive transhalogenation reaction described above. Preliminary radiolabelling experiments showed that 30–45 min was the optimal reaction time for this biotransformation, at which point the enzyme was cleanly heat-precipitated, diluted and removed by centrifugation. The lysate was then subjected to semi-prep HPLC and the peak corresponding to [^{18}F]**16** was collected (free of **15**, see Fig. S26–27†). The collected fraction was diluted with water and loaded onto a C18 reverse phase cartridge and after a wash with water, [^{18}F]**16** was eluted from the cartridge with EtOH. The purity of [^{18}F]**16** was determined by analytical radio-HPLC (see Fig. 3), and its identity further confirmed by examination of a sample spiked with FDA-PEG-GUL **16** (see Fig. S27a†). A typical procedure from [^{18}F]fluoride (572 MBq) to [^{18}F]**16** (19.2 MBq) elution in EtOH took 1.5 h, and afforded a radiochemical yield of ~3.4% (decay uncorrected) and a radiochemical purity of >99%. This yield is in line with that reported for other fluorinase catalysed radiolabelling. The success of this protocol, along with the robust nature of the fluorinase, allows for its further development and the potential incorporation of immobilised enzyme. In such an instance,

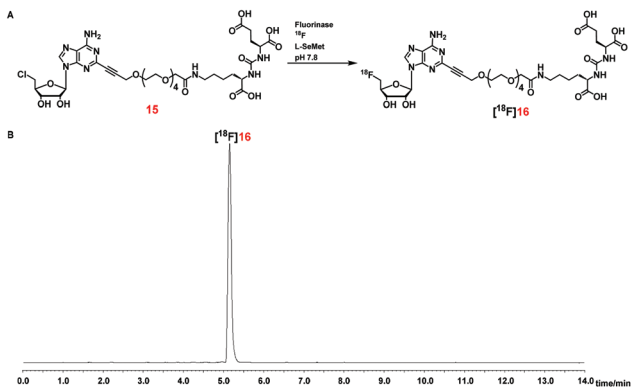

Fig. 3 (A) Reaction scheme of the fluorinase catalysed transhalogenation of **15** to [^{18}F]FDA-PEG-GUL ([^{18}F]**16**). (B) Analytical HPLC radio trace of [^{18}F]FDA-PEG-GUL ([^{18}F]**16**) after purification. For additional information on HPLC set up and conditions for radiolabelling experiments see ESI.†

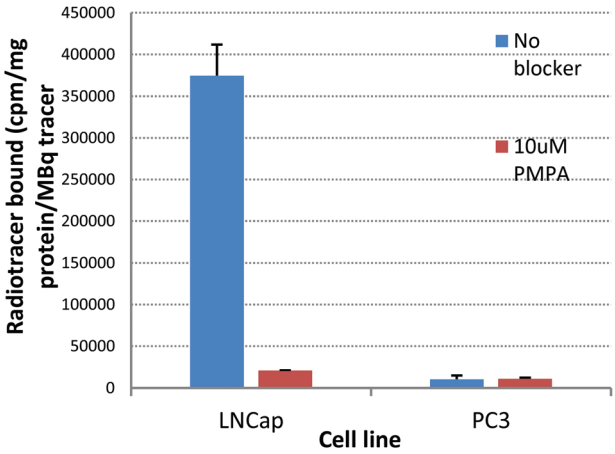

Fig. 4 Bound [^{18}F]**16** [cpm mg^{-1}] protein per MBq radiotracer.

the methodology could be then integrated into an automated system which utilises greater amounts of [^{18}F]fluoride to increase the scale and yields of [^{18}F]**16** production.

Specific cell binding of [^{18}F]FDA-PEG-GUL 16 to PSMA expressing cancer cells

The binding of [^{18}F]**16** to PSMA on the surface of cancer cells was evaluated in LNCaP (which are well known to express high levels of PSMA) and PC3 (which do not express PSMA) cell lines.[45] Western blotting analysis of cell lysates confirmed that the LNCaP cells used in this study expressed PSMA, whereas the PC3 cells did not (data not shown). A high level of [^{18}F]**16** binding was observed in LNCaP cells (Fig. 4), but not in PC3 cells. 2-PMPA (10 μM) was included in binding assays to permit identification of specific radiotracer binding to PSMA from non-specific binding. Inclusion of 2-PMPA decreased [^{18}F]**16** binding to LNCaP cells by approximately 95%, but had no effect on radiotracer binding to PC3 cells (Fig. 4). These data are consistent with the non-radiolabelled inhibition assay and provide strong support that [^{18}F]**16** binds selectively to PMSA in prostate cancer cells.

Conclusions

This study established FDA-PEG-GUL **16** as a new low molecular weight PSMA-targeting ligand, which was generated using the fluorinase enzyme by biotransformation from its chlorinated precursor ClDA-PEG-GUL **15**, further extending the repertoire of substrates accepted by this enzyme. FDA-PEG-GUL **16** was utilised for *in vitro* studies and found to be a potent inhibitor of the PSMA protein. As part of this study, a protocol was developed to allow for the enzymatic production of [^{18}F]FDA-PEG-GUL ([^{18}F]**16**), making it a potential new PET radiotracer for imaging prostate cancer. Candidate tracer [^{18}F]**16** was evaluated in a cell-based assays and demonstrated to selectively bind to cells expressing PSMA.

Experimental

Non-radioactive transhalogenation assay

In a total reaction volume of 1000 μL (in 50 mM phosphate buffer, at pH 7.8), recombinant fluorinase (0.8 mg mL^{-1}) was incubated with ClDA-PEG-GUL **15** (0.08 mM), L-SeMet (0.075 mM) and KF (50 mM) at 37 °C. Samples (50 μL) were periodically removed, the protein precipitated by heating at 95 °C for 5 min, before being clarified by centrifugation (13 000 rpm, 10 min). Samples of the supernatant (40 μL) were removed for analysis by HPLC, which was performed on a Shimadzu Prominence system using a Kinetix 5 μm XB-C18 100A (150 mm × 4.6 mm) column and a guard cartridge. Mobile phase: 0.05% TFA in water (solvent A) and 0.05% TFA in MeCN (solvent B); linear gradient: 15% solvent B to 95% solvent B over 25 min, 95% for 5 min, and back to 15% B for 10 min to re-equilibrate the column. Flow rate: 1 mL min^{-1}; detection: 254 nm; injection volume: 40 μL.

^{18}F-labelling of 15 to [^{18}F]16

A typical ^{18}F-labelling experiment of **15** was performed as follows: L-SeMet (40 μL of a 2 mM solution in water) and compound **15** (0.2 mg in 40 μL of water) were added successively to an Eppendorf tube containing a solution of fluorinase (5 mg in 50 mm phosphate buffer, 80 μL). The contents were mixed well with a pipette and to this mixture was added [^{18}F]fluoride in [^{18}O]water (572 MBq, 80 μL), making a total volume of 240 μL. The contents were again well mixed and incubated at 37 °C for 45 min. After this time, the reaction was stopped, the mixture denatured by heating at 95 °C for 5 min and water (250 μL) added before being clarified by centrifugation (13 000 rpm, corresponding to 16 060*g*, 5 min). The supernatant was injected into a Shimadzu Prominence HPLC system equipped with a quaternary pump, a degasser, a flow cell detector and a diode array detector using a Phenomenex Kingsorb C18 (250 × 10 mm, 5 μm) column and a guard cartridge. Mobile phase: 0.05% TFA in water (solvent A) and 0.05% TFA in MeCN (solvent B); linear gradient: 15% solvent B to 38% solvent B over 16 min, 95% for 5 min, and back to 15% B for 10 min to re-equilibrate the column. Flow rate: 2.5 mL min^{-1}. The radioactive fraction corresponding to the reference of [^{18}F]**16** was collected, diluted with water (50 mL) and loaded onto a pre-activated Waters Oasis HLB® Cartridge (conditioned with 2 mL EtOH and 5 mL water). The cartridge was washed with 20 mL of water and the desired product was collected by eluting with 1 mL of ethanol, to give 19.2 MBq (3.4%, decay uncorrected) of >99% pure product of [^{18}F]**16**.

Conflicts of interest

There are no conflicts of interest to declare.

Acknowledgements

We thank the Engineering and Physical Sciences Research Council, UK, for a research grant (EP/M01262X/1).

Notes and references

1 F. Bray, J. Ferlay, I. Soerjomataram, R. L. Siegel, L. A. Torre and A. Jemal, *CA-Cancer J. Clin.*, 2018, **68**, 394–424.
2 G. L. Andriole, E. D. Crawford, R. L. Grubb, S. S. Buys, D. Chia, T. R. Church, M. N. Fouad, E. P. Gelmann, P. A. Kvale, D. J. Reding, J. L. Weissfeld, L. A. Yokochi, B. O'Brien, J. D. Clapp, J. M. Rathmell, T. L. Riley, R. B. Hayes, B. S. Kramer, G. Izmirlian, A. B. Miller, P. F. Pinsky, P. C. Prorok, J. K. Gohagan and C. D. Berg, *N. Engl. J. Med.*, 2009, **360**, 1310–1319.
3 R. L. Siegel, K. D. Miller and A. Jemal, *CA-Cancer J. Clin.*, 2018, **68**, 7–30.
4 M. I. Davis, M. J. Bennett, L. M. Thomas and P. J. Bjorkman, *Proc. Natl. Acad. Sci. U. S. A.*, 2005, **102**, 5981–5986.
5 M. A. Meighan, M. T. Dickerson, O. Glinskii, V. V. Glinsky, G. L. Wright and S. L. Deutscher, *J. Protein Chem.*, 2003, **22**, 317–326.
6 C. Barinka, J. Starkova, J. Konvalinka and J. Lubkowski, *Acta Crystallogr., Sect. F: Struct. Biol. Cryst. Commun.*, 2007, **63**, 150–153.
7 J. T. Pinto, B. P. Suffoletto, T. M. Berzin, C. H. Qiao, S. Lin, W. P. Tong, F. May, B. Mukherjee and W. D. Heston, *Clin. Cancer Res.*, 1996, **2**, 1445–1451.
8 M. B. Robinson, R. D. Blakely, R. Couto and J. T. Coyle, *J. Biol. Chem.*, 1987, **262**, 14498–14506.
9 G. D. Ghadge, B. S. Slusher, A. Bodner, M. D. Canto, K. Wozniak, A. G. Thomas, C. Rojas, T. Tsukamoto, P. Majer, R. J. Miller, A. L. Monti and R. P. Roos, *Proc. Natl. Acad. Sci. U. S. A.*, 2003, **100**, 9554–9559.
10 J. Zhou, J. H. Neale, M. G. Pomper and A. P. Kozikowski, *Nat. Rev. Drug Discovery*, 2005, **4**, 1015.
11 A. Ghosh and W. D. Heston, *J. Cell. Biochem.*, 2004, **91**, 528–539.
12 D. G. Bostwick, A. Pacelli, M. Blute, P. Roche and G. P. Murphy, *Cancer*, 1998, **82**, 2256–2261.
13 S. Perner, M. D. Hofer, R. Kim, R. B. Shah, H. Li, P. Moller, R. E. Hautmann, J. E. Gschwend, R. Kuefer and M. A. Rubin, *Hum. Pathol.*, 2007, **38**, 696–701.
14 K. Rahbar, A. Afshar-Oromieh, H. Jadvar and H. Ahmadzadehfar, *Mol. Imaging*, 2018, **17**, 1536012118776068–1536012118776068.
15 S. Zschaeck, F. Lohaus, M. Beck, G. Habl, S. Kroeze, C. Zamboglou, S. A. Koerber, J. Debus, T. Hölscher, P. Wust, U. Ganswindt, A. D. J. Baur, K. Zöphel, N. Cihoric, M. Guckenberger, S. E. Combs, A. L. Grosu, P. Ghadjar and C. Belka, *Radiat. Oncol.*, 2018, **13**, 90.

16 A. G. Thomas, K. M. Wozniak, T. Tsukamoto, D. Calvin, Y. Wu, C. Rojas, J. Vornov and B. S. Slusher, *Adv. Exp. Med. Biol.*, 2006, **576**, 327–337.
17 D. V. Ferraris, K. Shukla and T. Tsukamoto, *Curr. Med. Chem.*, 2012, **19**, 1282–1294.
18 P. F. Jackson, D. C. Cole, B. S. Slusher, S. L. Stetz, L. E. Ross, B. A. Donzanti and D. A. Trainor, *J. Med. Chem.*, 1996, **39**, 619–622.
19 P. Majer, P. F. Jackson, G. Delahanty, B. S. Grella, Y.-S. Ko, W. Li, Q. Liu, K. M. Maclin, J. Poláková, K. A. Shaffer, D. Stoermer, D. Vitharana, E. Y. Wang, A. Zakrzewski, C. Rojas, B. S. Slusher, K. M. Wozniak, E. Burak, T. Limsakun and T. Tsukamoto, *J. Med. Chem.*, 2003, **46**, 1989–1996.
20 B. Grella, J. Adams, J. F. Berry, G. Delahanty, D. V. Ferraris, P. Majer, C. Ni, K. Shukla, S. A. Shuler, B. S. Slusher, M. Stathis and T. Tsukamoto, *Bioorg. Med. Chem. Lett.*, 2010, **20**, 7222–7225.
21 D. Stoermer, Q. Liu, M. R. Hall, J. M. Flanary, A. G. Thomas, C. Rojas, B. S. Slusher and T. Tsukamoto, *Bioorg. Med. Chem. Lett.*, 2003, **13**, 2097–2100.
22 C. Barinka, Y. Byun, C. L. Dusich, S. R. Banerjee, Y. Chen, M. Castanares, A. P. Kozikowski, R. C. Mease, M. G. Pomper and J. Lubkowski, *J. Med. Chem.*, 2008, **51**, 7737–7743.
23 W. P. Fendler, C. Bluemel, J. Czernin and K. Herrmann, *Clin. Trans. Imaging*, 2016, **4**, 467–472.
24 E. Gourni and G. Henriksen, *Molecules*, 2017, **22**, 523.
25 K. Kopka, M. Benesova, C. Barinka, U. Haberkorn and J. Babich, *J. Nucl. Med.*, 2017, **58**, 17S–26S.
26 H. Wang, Y. Byun, C. Barinka, M. Pullambhatla, H. E. Bhang, J. J. Fox, J. Lubkowski, R. C. Mease and M. G. Pomper, *Bioorg. Med. Chem. Lett.*, 2010, **20**, 392–397.
27 M. Eder, M. Schäfer, U. Bauder-Wüst, W.-E. Hull, C. Wängler, W. Mier, U. Haberkorn and M. Eisenhut, *Bioconjugate Chem.*, 2012, **23**, 688–697.
28 O. Mawlawi and D. W. Townsend, *Eur. J. Nucl. Med. Mol. Imaging*, 2009, **36**(Suppl 1), S15–S29.
29 V. Bouvet, M. Wuest, J. J. Bailey, C. Bergman, N. Janzen, J. F. Valliant and F. Wuest, *Mol. Imaging Biol.*, 2017, **19**, 923–932.
30 J. L. Sutcliffe-Goulden, M. J. O'Doherty, P. K. Marsden, I. R. Hart, J. F. Marshall and S. S. Bansal, *Eur. J. Nucl. Med. Mol. Imaging*, 2002, **29**, 754–759.
31 S. Robu, A. Schmidt, M. Eiber, M. Schottelius, T. Gunther, B. Hooshyar Yousefi, M. Schwaiger and H. J. Wester, *EJNMMI Res.*, 2018, **8**, 30.
32 N. Malik, B. Baur, G. Winter, S. N. Reske, A. J. Beer and C. Solbach, *Mol. Imaging Biol.*, 2015, **17**, 777–785.
33 S. Boschi, J. T. Lee, S. Beykan, R. Slavik, L. Wei, C. Spick, U. Eberlein, A. K. Buck, F. Lodi, G. Cicoria, J. Czernin, M. Lassmann, S. Fanti and K. Herrmann, *Eur. J. Nucl. Med. Mol. Imaging*, 2016, **43**, 2122–2130.
34 J. Giglio, M. Zeni, E. Savio and H. Engler, *EJNMMI Radiopharmacy Chem.*, 2018, **3**, 4.
35 D. O'Hagan, C. Schaffrath, S. L. Cobb, J. T. G. Hamilton and C. D. Murphy, *Nature*, 2002, **416**, 279–279.
36 C. Dong, F. Huang, H. Deng, C. Schaffrath, J. B. Spencer, D. O'Hagan and J. H. Naismith, *Nature*, 2004, **427**, 561–565.
37 H. Deng, S. L. Cobb, A. R. McEwan, R. P. McGlinchey, J. H. Naismith, D. O'Hagan, D. A. Robinson and J. B. Spencer, *Angew. Chem., Int. Ed.*, 2006, **45**, 759–762.
38 S. Thompson, Q. Zhang, M. Onega, S. McMahon, I. Fleming, S. Ashworth, J. H. Naismith, J. Passchier and D. O'Hagan, *Angew. Chem., Int. Ed.*, 2014, **53**, 8913–8918.
39 S. Thompson, I. N. Fleming and D. O'Hagan, *Org. Biomol. Chem.*, 2016, **14**, 3120–3129.
40 Q. Zhang, S. Dall'Angelo, I. N. Fleming, L. F. Schweiger, M. Zanda and D. O'Hagan, *Chem. – Eur. J.*, 2016, **22**, 10998–11004.
41 P. T. Lowe, S. Dall'Angelo, T. Mulder-Krieger, A. P. Ijzerman, M. Zanda and D. O'Hagan, *ChemBioChem*, 2017, **18**, 2156–2164.
42 P. T. Lowe, S. Dall'Angelo, A. Devine, M. Zanda and D. O'Hagan, *ChemBioChem*, 2018, **19**, 1969–1978.
43 T. Wustemann, U. Bauder-Wust, M. Schafer, M. Eder, M. Benesova, K. Leotta, C. Kratochwil, U. Haberkorn, K. Kopka and W. Mier, *Theranostics*, 2016, **6**, 1085–1095.
44 R. Luthi-Carter, A. K. Barczak, H. Speno and J. T. Coyle, *Brain Res.*, 1998, **795**, 341–348.
45 S. S. Chang, V. E. Reuter, W. D. Heston, N. H. Bander, L. S. Grauer and P. B. Gaudin, *Cancer Res.*, 1999, **59**, 3192–3198.